



Original Paper

Mobilization of tight oil by spontaneous imbibition of surfactants

Ming-Chen Ding^{a, b, c, *}, Xin-Fang Xue^c, Ye-Fei Wang^{a, b, c}, Chu-Han Zhang^{a, b, c}, Shi-Ze Qiu^{a, b, c}^a State Key Laboratory of Deep Oil and Gas, China University of Petroleum (East China), Qingdao, 266580, Shandong, PR China^b Key Laboratory of Unconventional Oil & Gas Development (China University of Petroleum (East China)), Ministry of Education, Qingdao, 266580, Shandong, PR China^c School of Petroleum Engineering, China University of Petroleum (East China), Qingdao, 266580, Shandong, PR China

ARTICLE INFO

Article history:

Received 16 June 2024

Received in revised form

24 August 2024

Accepted 28 August 2024

Available online 29 August 2024

Edited by Yan-Hua Sun

Keywords:

Tight oil

Spontaneous imbibition

Surfactant

Oil mobilization

Visual research

ABSTRACT

A series of spontaneous imbibition (SI) tests of tight oil were performed, together with oil distribution scans by computed tomography (CT) and nuclear magnetic resonance (NMR). Thus, the best surfactants to optimize the SI effect were obtained, the basic requirements to surfactants for efficient SI were determined, and the oil mobilization by SI revealed. The results show that anionic surfactants significantly outperform non-ionic, cationic, and zwitterionic ones in SI process. Excellent systems can be further obtained by mixing anionic surfactants with others (e.g. 1:1 mixtures of AES:EHSB). The requirements to interfacial properties of surfactants for achieving efficient SI at permeabilities of 0.05, 0.5, and 5.0 mD are as follows: 10^0 mN/m, $< 40^\circ$; 10^{-1} – 10^0 mN/m, $< 55^\circ$; and 10^{-1} – 10^0 mN/m, $< 70^\circ$, respectively. Although a high oil recovery of 38.5% by SI was achieved in small cylindrical cores ($\phi 2.5$ cm \times 3.0 cm), the joint SI and CT tests in larger, cube-shaped cores (5.0 cm \times 5.0 cm \times 5.0 cm) showed that the SI process could only remove the oil from the outermost few millimeters of the cores with permeabilities of 0.05 and 0.1 mD, indicating the great difficulty encountered for their development. The NMR showed that the SI treatment preferentially removed oil from smaller pores rather than medium or large pores.

© 2024 The Authors. Publishing services by Elsevier B.V. on behalf of KeAi Communications Co. Ltd. This is an open access article under the CC BY-NC-ND license (<http://creativecommons.org/licenses/by-nc-nd/4.0/>).

1. Introduction

With super-high water cuts and low oil production rates, it becomes increasingly difficult for the development of conventional oil reservoirs, 'tight oil' reservoirs have been much focused upon around the world due to the vast reserves they contain. Tight oil generally refers to oil aggregations with matrix permeabilities not greater than 0.1 mD (air permeability less than 1.0 mD) and porosity less than 10% (Jia et al., 2012). According to the Energy Information Administration, there are 4.73×10^{10} tons of recoverable tight oil reserves around the world and this oil may account for 45% of the total worldwide oil production by 2035 (Sieminsk et al., 2013). However, the tight nature of these reservoirs makes it difficult to inject them with water (the traditional approach to extraction), and for the tight oil to flow out. The application of

horizontal well and volumetric fracturing has successfully enabled some tight oil to be produced. However, single-well production is low and the rate of oil production rapidly declines; the development of such sources is consequently severely limited (Chaudhary et al., 2011; Zhang et al., 2015). The yield from a single well usually drops to less than 20% of its initial value within a year. Moreover, the oil recovered by the primary elastic exploitation process is only 5%–10% (some scholars believe that this could even be as low as 1%–2%) (Fragoso et al., 2018; Sheng, 2015).

Finding strategies to effectively recover more tight oil is therefore of paramount importance. In this context, it is important to remember that water injection is considered to be the most appropriate way of carrying out hydraulic fracturing. Indeed, water flooding and huff-and-puff have been employed in Bakken wells (USA and Canada) (Todd and Evans, 2016; Kiani et al., 2019) and tight blocks in the Changqing and Daqing oilfields (China), and some progress has been made. Spontaneous imbibition (SI) is believed to be one of the keys to removing tight oil via such water-based technologies. During the imbibition process, water (as a

* Corresponding author. State Key Laboratory of Deep Oil and Gas, China University of Petroleum (East China), Qingdao, 266580, Shandong, PR China.

E-mail address: Dingmc@upc.edu.cn (M.-C. Ding).

wetting phase) is imbibed into the tight matrix by capillary forces or buoyancy, thus displacing the oil (as a non-wetting phase), allowing it to be recovered (Cheng et al., 2019; Ren et al., 2023; Tian et al., 2023). To enhance the imbibition process, a surfactant or other interface-active substance is usually added to the water to help change the rock's wettability and reduce interfacial tension (IFT) (Jia et al., 2022; Liu and Sheng, 2019; Wei et al., 2023; Zhu et al., 2023). It is believed that the capillary pressure shifts from negative to positive when the wettability shifts from oil-wet to water-wet (which is conducive to SI). On the other hand, the lower the IFT, the easier it is for crude oil to be shed from the rock and flow out. A great deal of work has been carried out on optimizing potential SI agents, elucidating SI micro-mechanisms, and determining the oil mobilization characteristics of the SI process, etc. (Wang et al. 2012, 2019; Jiang et al., 2023; Dai et al., 2019; Shuler et al., 2011; Sheng, 2017; Neog and Schechter, 2016; Alvarez et al., 2014, 2017; Zhao et al., 2022). Nevertheless, there are still some urgent problems that need resolving when surfactant-assisted SI is applied to tight oil recovery.

Firstly, we need to determine what kinds of surfactant should be used to maximize the SI effect in tight oil reservoirs. In other words, as surfactants have certain characteristic abilities (especially, in the current context, to alter wettability and reduce IFT), what are the optimum levels of these abilities as far as recovering tight oil is concerned? Shuler et al. (2011) and Wang et al. (2012) compared the ability of various types of surfactants to recover shale oil from middle Bakken wells. Some promising surfactants were identified, but further clarification of what makes these surfactants the best (in terms of their properties) was not given. On the other hand, Liu and Sheng (2019), investigating surfactant-enhanced SI in Chinese shale oil reservoirs, concluded that the surfactant's ability to affect wettability is the key to enhancing oil recovery (that is, IFT reduction was found to be unimportant). It has been found that if a surfactant cannot change the wettability state of the rock from oil-wet to water-wet, mass transfer cannot occur between the matrix and fractures (so no oil can be produced via the SI process) regardless of the IFT value (Sheng, 2017). Neog and Schechter (2016) found that surfactants that could significantly affect wettability and slightly reduce the IFT performed best in their SI experiments using Wolfcamp shale. Having a very low IFT is unfavorable as IFT reduction lowers the effectiveness with which wettability alteration is able to enhance oil recovery using SI. It has been suggested that ultra-low IFT values favor the redeposition of oil onto the rock surface and movement of water out of the matrix due to the capillary pressure approaching zero (Alvarez et al., 2014, 2017). However, other workers continue to emphasize that ultra-low IFT has a role to play in the successful SI of tight oil. For example, Zhao et al. (2022) developed a surfactant–silica nanoparticle system to enhance oil recovery from reservoirs with ultra-low permeability. Their system, which yielded an ultra-low IFT of 3.18×10^{-3} mN/m, could remove a very significant recovery rate (28.5%) of the oil via imbibition. Similarly, Jia et al. (2022) selected an ultra-low-IFT zwitterionic surfactant for imbibition-enhanced oil recovery from tight reservoirs. They concluded that the stronger the change in wettability and the lower the IFT of the imbibition fluid, the greater the oil recovery rate. Xiao et al. (2022) used a microemulsion system to enhance imbibition in tight, ultra-low-permeability reservoirs, and attributed its beneficial action to its ultra-low IFT and strong wettability alteration effect. In contrast, Dou et al. (2021) found that in the case of dynamic imbibition, the oil recovery rate increases to begin with as the IFT decreases and then decreases, implying there is an optimal IFT value at which the oil recovery rate is maximal. Guo et al. (2020) investigated SI in tight sandstone reservoirs and came to the conclusion that it is not the case that the smaller the IFT the better. Again, this suggests an

optimal value exists that maximizes the ultimate level of imbibition recovery. In general, capillary pressure is proportional to the IFT value. Therefore, increasing IFT will lead to an increase in the key force that drives SI. However, lower IFT makes it easier to displace the oil from the surface of the rock. The abovementioned experimental results suggest there is some uncertainty in the effect that IFT has on SI. This can make it highly confusing when it comes to designing and selecting surfactants for use in tight oil imbibition. Therefore, in this paper, the surfactants used in tight oil SI experiments are first optimized. More importantly, the basic characteristics of the 'good' surfactants that give the best SI effects in tight oil reservoirs are then revealed.

In addition to the SI agents discussed above, the characteristics of the oil mobilization induced by the SI are also focused, especially the removal of oil from pores of different sizes. Ren et al. (2023) found that, although the macropores dominated the oil recovery process, the mesopores and micropores also play a crucial role and their maximum oil recovery actually surpassed that of the former. Cheng et al. (2019) concluded that the oil recovered as a result of imbibition mainly comes from the contribution made by sub-micropores, i.e. micropores only make a minor contribution to the total oil recovered. Gu et al. (2017) concluded that micron-sized and larger pores contribute greatly to the imbibition recovery process (while nano-sized pores make very little contribution). Yang et al. (2019) suggested that oil and water exchange is first realized in the micropores as these have the smallest size and largest capillary force (thus yielding the highest oil recovery rate during SI). They further suggested that the residual oil is mainly distributed in the mesopores (i.e. pores with diameters in the range 0.03–0.1 μm). However, there is a key question to answer before studying the oil recovery rate from pores with different sizes: can the water and surfactant flowing in the hydraulic-fracturing-induced fractures effectively penetrate deep inside tight matrices when SI is employed? Alternatively phrased, to what depth is SI able to exhaust the crude oil from a tight matrix? In this context, it is important to remember that hydraulic fracturing in actual tight reservoirs cannot cut the rock into units as small as the cores used in experiments. As a result, the recovery of oil from actual reservoirs can hardly approach the values measured experimentally in the lab. Liu et al. (2024) recognized that, as the core size increases (i.e. fractures are less well-developed), the degree of pore mobilization decreases for all pore sizes. So, rather than the oil recovery rate from small cores using SI in the laboratory, it is the activation depth achieved that gives a more accurate reflection of the discharge effect to be expected in real oil reservoirs. In other words, if the activation depth using SI is very limited, then (even if crude oil can be expelled from pores of all sizes) it is difficult to achieve a good rate of oil recovery from the reservoir. In fact, people have already begun to notice the impact of this size effect. Yang et al. (2019) estimated the imbibition distance by comparing the flow resistance of the oil phase before and after carrying out water-flooding huff and puff imbibition experiments. In cores with a permeability of 0.2 mD, the imbibition distance was found to be 30.4 cm. On the other hand, Qi et al. (2023) used a computed tomography (CT) method to study the countercurrent imbibition distance in cores with permeabilities in the range 0.3–0.7 mD and found it to be just a few centimeters. Apart from these assessments, experiments aimed at determining the imbibition depth of oil in tight rock specimens are very limited. Further investigation is therefore urgently required.

In this paper, the results of a large number of tight oil SI tests are reported. They were conducted using a total of 44 surfactants belonging to 6 categories (anionic, cationic, non-ionic, zwitterionic, combined, and commercial). Almost all of the types of surfactants commonly used in oil fields are covered (because we currently do

not know exactly what the most effective combination of surfactant properties is). Based on the measured SI recovery data, the optimal surfactant to use to enhance the recovery rate of tight oil using SI is then deduced. More importantly, correlation analysis can be used to reveal which surfactant properties are most important for enhancing the recovery of tight oil. The results should, therefore, help engineers design and select the most efficient surfactant to use in particular tight oil reservoirs. In addition to the SI tests, the characteristics of the oil distributions in the cores were scanned and visualized using CT before and after performing the surfactant-assisted SI tests. This is to allow us to intuitively observe and judge the true activation depth of the tight oil achieved using different surfactants.

2. Experimental

2.1. Materials

A light, translucent crude oil that had been collected from a tight oil reservoir was acquired from the China National Petroleum Corporation (CNPC) and used for all the SI tests performed in this work. The density and viscosity of the oil were found to be 800.0 kg/m³ and 2.7 mPa s (measured at 80 °C and 0.101 MPa), respectively. The anionic, non-ionic, and zwitterionic surfactants employed were obtained from the Shandong Linyi Lusun Chemical Co., Ltd; the cationic ones were all purchased from the Sinopharm Chemical Reagent Co., Ltd and were of a chemically pure grade. The ‘combined’ surfactants mentioned above are simply mixtures of two or three of the other surfactants: the details of their compositions are specified in Table 1.

The commercial surfactants used for comparison purposes were developed and produced by several companies with the aim of enhancing the imbibition of tight oil. The surfactants ULOB50, 04A, and F1209 were provided by the Zibo Yonghong New Material Co., Ltd; 5231 was from the Tianjin Xiongguan Technology Development Co., Ltd; TG 902 and NBI were produced by CNPC Engineering Materials Research Institute Co., Ltd; LG300 was provided by the Shanghai Futian Chemical Technology Co., Ltd; and DMI was acquired from the Shandong Daming Environmental Protection Engineering Technology Co., Ltd. This research initially intended to

use just these surfactants to enhance the imbibition effect, so their solutions were prepared in water containing 0.02% NaCl (to simulate the salinity of the water used to prepare fracturing fluid in the field). The concentration of each surfactant evaluated was maintained at a common value (0.3%) in all of the experiments conducted.

A kind of epoxy-cemented quartz sandstone core (widely used in the EOR field) was used in the SI experiments, with an initial, nearly neutral wetting surface (contact angle 89°). Those cores were designed to be differential sizes (cylindrical cores: ϕ 2.5 cm \times 3.0 cm; cubic cores: 5.0 cm \times 5.0 cm \times 5.0 cm) and permeability (0.005–30 mD) for different experimental purposes.

2.2. Experimental methods and setup

2.2.1. Contact angle and IFT measurement

The contact angle (CA, θ) is the main index used to specify the wettability of a rock surface. According to a widely accepted standard, $\theta > 90^\circ$ corresponds to an oil-wet surface, $\theta = 90^\circ$ to intermediate wettability, and $\theta < 90^\circ$ to a water-wet surface. In this study, the CAs of the cores were measured before and after performing their imbibition tests. The specific steps employed were as follows: (i) Cores were first vacuumized for 3 h and then saturated with oil for 14 days at 80 °C. The oil was pressurized to 20 MPa during this period. This was to ensure the tight cores were fully saturated with oil and to allow them to age to improve the oil wettability of the pore surfaces. (ii) A needle was then used to transfer a drop of the simulated water onto the surface of the test core. The initial CA of the surface was then measured using a contact angle meter (model SL200KB, made in China) at 20 °C. The CA was found to have an average value of 117°. (iii) The cores were then soaked in pure water or surfactant solution for about 90–116 h. A water droplet was then again placed onto the surface of the test core and its CA value was determined again. The ability of the different surfactants to alter the wettability of the core surface was thus determined (Table 1).

The IFT between each surfactant and tight oil was measured using a rotating drop IFT meter (model TX500C, made in China) at a rotation speed of 3000 r/min and temperature of 80 °C. The meter used was equipped with an image-capturing device and image-

Table 1
Interfacial properties of the surfactants used in the experiments and their corresponding SI recovery rates (using cores with permeabilities of ~0.5 mD).

No.	SI fluid	IFT, mN/m	CA, °	SI recovery, %	No.	SI fluid	IFT, mN/m	CA, °	SI recovery, %		
1	Water	20.30	89.0	8.1	24	Combined	AES:EHSB:APG/3:1:2	0.71	37.9	32.8	
2	Anionic	AES	2.07	30.2	27.6	25	AES:EHSB:APG/5:3:4	0.82	43.3	33.1	
3		ALS	1.74	36.4	22.5	26	AES:EHSB:APG/1:1:1	0.34	52.1	30.0	
4		SLS	1.77	33.6	26.5	27	AES:EHSB:APG:6501/3:1:1:1	1.24	33.8	19.2	
5		SDBS	0.64	0.0	25.2	28	AES:EHSB:6501/1:1:1	0.005	70.6	12.8	
6		SDS	2.06	69.7	21.1	29	SDBS:EHSB/3:1	0.13	20.9	36.4	
7	Cationic	CTAB	0.10	97.2	0.8	30	SDBS:EHSB/5:3	0.25	34.9	29.0	
8		DTAB	0.43	92.7	0.7	31	SDBS:EHSB/1:1	0.14	31.1	38.1	
9		DTAC	0.70	96.5	0.0	32	SDBS:EHSB:APG/3:1:2	0.18	33.0	25.5	
10	Zwitterionic	BS-12	0.93	64.4	1.5	33	SDBS:EHSB:APG/5:3:4	0.11	31.8	38.5	
11		BS-18	0.20	87.2	0.4	34	SDBS:EHSB:APG/1:1:1	0.22	25.8	34.5	
12		CHSB	0.12	86.8	0.4	35	SDBS:EHSB:APG:6501/3:1:1:1	0.35	29.9	31.3	
13		DHSB	0.17	97.3	0.4	36	SDBS:EHSB:6501/1:1:1	0.001	56.5	21.1	
14		EAB	0.08	88.6	0.4	37	Commercial	ULOB50	0.44	34.8	31.2
15		EHSB	0.07	67.9	2.4	38	04A	0.18	40.2	28.2	
16		OAB	0.21	89.3	0.4	39	F1209	0.40	25.7	30.3	
17	Non-ionic	6501	0.21	0.0	19.6	40	5231	0.0068	35.6	23.1	
18		Tween-80	0.37	27.8	18.2	41	PEG	0.21	34.8	27.8	
19		APG0810	0.47	45.5	20.0	42	TG902	0.0017	17.9	23.9	
20		TX-100	0.48	70.7	18.4	43	NBI	0.18	22.4	27.7	
21	Combined	AES: EHSB/3:1	1.79	24.7	28.6	44	LG300	0.13	27.3	30.8	
22		AES: EHSB/5:3	0.93	38.9	35.8	45	DMI	0.02	15.1	18.5	
23		AES: EHSB/1:1	0.62	37.7	38.5						

acquisition software, allowing it to automatically measure and record the dynamic IFT. For this work, the stable IFT of the surfactant–oil system was recorded about 2 h after the test was started. The results are shown in Table 1.

2.2.2. Imbibition tests

SI tests were conducted on the cores at 80 °C using Amott cells (Fig. 1). The test core was placed vertically in an Amott cell containing the surfactant solution to be tested (at a fixed concentration of 0.3%). SI resulted in oil being spontaneously removed from the core, the volume of which could then be measured using the scale in the upper part of the Amott cell. Two types of cores were used in the SI experiments: cylindrical ones measuring $\phi 2.5 \text{ cm} \times 3.0 \text{ cm}$ and cubic ones measuring $5.0 \text{ cm} \times 5.0 \text{ cm} \times 5.0 \text{ cm}$. The smaller, cylindrical cores were used to compare the SI recovery rates produced by different surfactants, find the optimal surfactant, and determine the basic requirements of the surfactant for efficient SI. The larger, cubic cores were used to determine the mobilization characteristics of the tight oil in response to the SI. This was accomplished by scanning the cores using CT equipment (SOMATOM Definition AS 128, Siemens, made in Germany) to determine the distribution pattern of the oil inside them.

The specific experimental procedure employed consisted of the following steps: (i) The cores were first cut into the pre-determined size and shape and then dried at 120 °C for 2 days to remove any residual water inside. The masses of the dried cores were subsequently measured and recorded. (ii) They were then placed into a pressure vessel and vacuumized for 3 h. Thereafter, oil was injected into the vessel and pressurized to 20 MPa. The cores were left for 14 days to become fully saturated with oil and to age at 80 °C. The masses of the cores were then recorded again. The mass of oil in each saturated core could then be found (and hence, by dividing by the known density of the oil, the volume of oil taken up by the core). (iii) The cores were subsequently placed in Amott cells and immersed in surfactant solution to start the imbibition process and be maintained for about 90–116 h. Throughout the SI process, the cells were maintained at 80 °C using a thermostatically-regulated water bath. (iv) The experiment was ended when the volume of oil produced in the measurement tube did not change for 24 h. (v)

The volume of oil discharged was recorded and used to calculate the SI recovery rate.

2.2.3. Oil-distribution scans

To determine the characteristics of the oil mobilization produced by the SI process, CT and nuclear magnetic resonance (NMR) scans were performed on the cores in tandem with the SI tests.

CT scans The CT technique is able to identify the distribution of oil and water in the core because the two liquids have different densities. However, to enhance signal contrast the density difference was increased by adding 15% KI to the water when preparing the surfactant solution. The addition of the KI did not have a significant effect on the essential properties of the surfactants used in this part of the research. For example, with the KI, the surfactants AES:EHSB (1:1) and TG902 were found to have IFT values of 0.85 and 0.0054 mN/m, respectively, which were very close to their IFT values in the absence of KI, 0.62 and 0.0017 mN/m, respectively. It was noteworthy that only these two surfactant solutions were used in the CT tests as they had the most SI promising performance.

The oil and water distributions in the tight cores were determined by subjecting them to CT scans at four distinct stages: at the beginning when the cores were dry, after they had been saturated with oil, after 1.5 h of SI, and after 134 h of SI. In this way, the distribution of the crude oil in the core during imbibition could be determined by comparing the signals captured at the different stages. The activation depth of the tight oil induced by the surfactant could then be elucidated. As previously mentioned, the cores employed in the CT experiments were the large cubic ones ($5.0 \text{ cm} \times 5.0 \text{ cm} \times 5.0 \text{ cm}$). These cores had permeabilities ranging from 0.005 to 30.0 mD in order to highlight the effect that the permeability of the core has on SI.

NMR scans The removal of oil from pores of different sizes was also investigated by analyzing the cores using a magnetic resonance scanner (model MicroMR12-150H, made in China). As the NMR signal was derived from the hydrogen nuclei in the fluids distributed throughout the core, a surfactant solution was prepared using deuterium water to shield the signal coming from the aqueous phase. Thus, only the oil phase was detected by the scanner. The cores were scanned twice, once at the initial oil-saturation stage

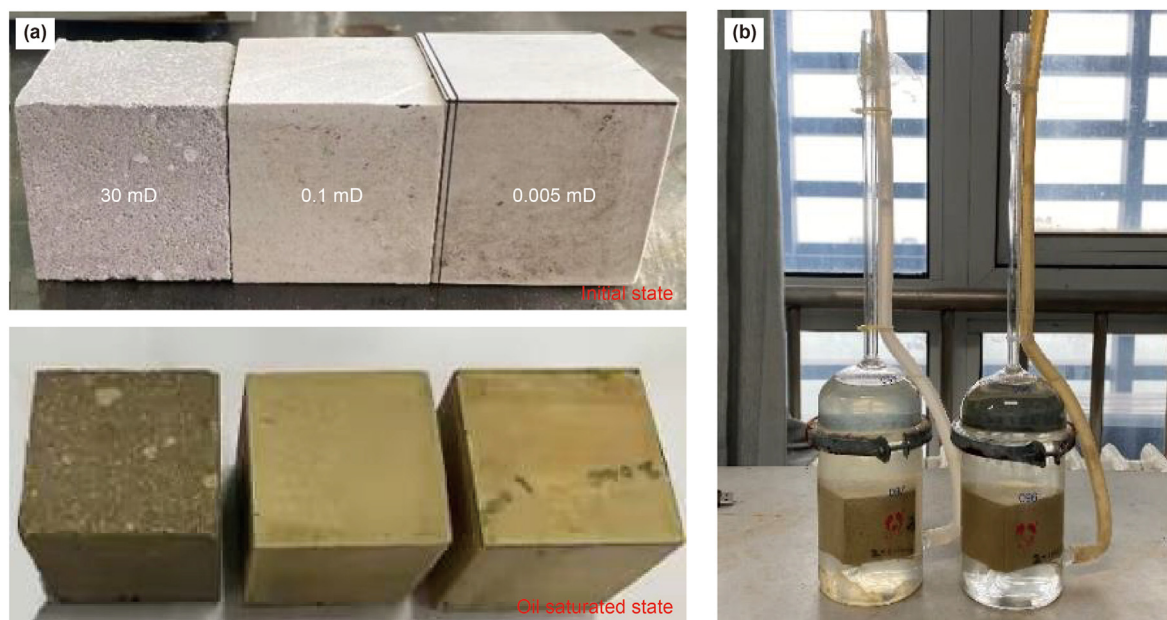


Fig. 1. (a) Cubic tight cores of different permeabilities before and after saturation with oil. (b) Photograph showing some of the Amott cells used to conduct the imbibition tests.

and once after imbibition. By comparing the transverse relaxation times (T_2) of the NMR signals before and after SI, how the proportions of oil stored in pores of different sizes change due to the SI process can be determined. The T_2 value essentially relates to the magnitude of the interaction between the nuclei in the oil and nuclei of the pore walls. In narrow pores, this interaction is strong and the NMR signal relaxes rapidly yielding a smaller T_2 value. Conversely, a large T_2 value corresponds to oil in wider pores.

Only the most effective surfactant, AES:EHSB (1:1), was used in the NMR experiments. Also, the cores used were the smaller cylindrical ones ($\phi 2.5 \text{ cm} \times 3.0 \text{ cm}$) with permeabilities in the range 0.005–5.0 mD.

3. Experimental results and discussion

3.1. Surfactant optimization

We first need to determine which surfactant is the most effective at displacing tight oil. However, despite an abundance of research on SI in the literature (including the mechanisms involved, which agents produce a good effect, factors influencing efficiency, etc.), it is still unclear what type of surfactant or what properties of surfactants should produce the most powerful SI effect in tight oil reservoirs. Some findings are even contradictory. Some people emphasize the importance of having an ultra-low IFT value (Liu and Sheng, 2019; Sheng, 2017; Neog and Schechter, 2016; Alvarez et al., 2014, 2017), while others think that it is the change in wettability (from oil-wet to water- or intermediate-wet) that is more important, regardless of the IFT value (Jia et al., 2022; Xiao et al., 2022; Zhao et al., 2022).

Hence, in this part of the work, the optimal surfactant for use in tight oil SI is obtained. As already stated, a total of 44 surfactants (anionic, cationic, non-ionic, zwitterionic, combined, and commercial) were collected, prepared, and evaluated. The results are shown in Table 1. The agents employed cover almost all the different types of surfactants commonly used in oil fields. This is essential as it is still unclear, in fact, exactly what kind of surfactant is most effective for the SI of tight oil.

3.1.1. Interfacial properties of single-component surfactants and their SI efficiency

The recovery rate of tight oil from the small, 0.5-mD cylindrical cores are first compared using the single-component surfactants

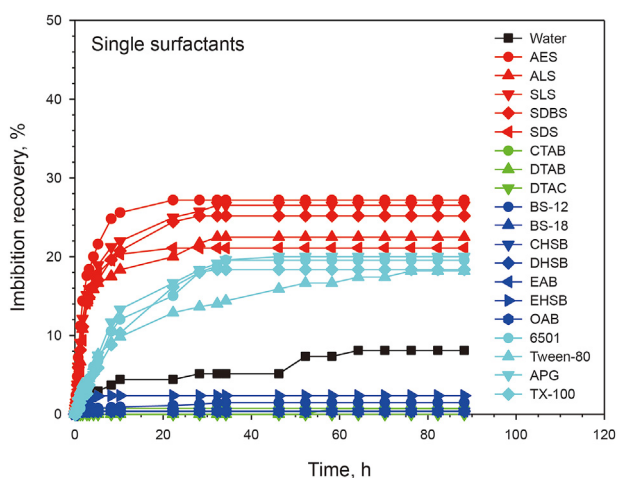


Fig. 2. Change in the SI recovery rate plotted as a function of time (single surfactants only). The data is colored according to surfactant type: red—anionic; cyan—non-ionic; blue—zwitterionic; green—cationic.

listed in Table 1 to achieve SI (Fig. 2). The results of their IFT and CA experiments are then examined to help understand why the different surfactants have different abilities to extract tight oil. In this way, the best single surfactant to use to displace tight oil via SI can be determined and rationalized.

As can be seen from Fig. 2 and Table 1, the SI recovery rate achieved using synthetic salt water is relatively low (8.1%) as the cores are oil-wet. The IFT value of the solution is clearly very high (20.3 mN/m) and the CA (89.0°) is also large, so the rock has intermediate wettability with respect to this solution. The solution's properties mean that the capillary pressure produced is insufficient to generate effective SI in the core. Consequently, it cannot discharge much of the oil from the core. Fig. 2 clearly illustrates that the efficiency of the SI process is strongly correlated with the basic nature of the surfactant (anionic, cationic, zwitterionic, etc.). To be more specific, the anionic surfactants (AES, ALS, SLS, SDDBS, and SDS) produced the highest rates of SI-mediated tight oil recovery: 21.1%–27.6%. In terms of orders of magnitude, the IFT values of these surfactants are roughly in the range of 10^{-1} – 10^0 mN/m, while their CA values are in the range of 0° – 69.7° . The next-best performing agents are the non-ionic surfactants (6501, Tween-80, APG0810, and TX-100) which managed to recover 18.2%–20.0% of the tight oil. The values of their IFTs and CAs are $\sim 10^{-1}$ mN/m and 0° – 70.7° , respectively. The cationic (CTAB, DTAB, and CTAC) and zwitterionic (BS-12, BS-18, CHSB, DHSB, EAB, EHSB, and OAB) surfactants performed very poorly (SI recovery rates of 0.4%–2.4%). Their IFTs and CAs are in the ranges of 10^{-2} – 10^{-1} mN/m and 64.4° – 97.3° , respectively. The performance of these agents was actually worse than that of the saline water, indicating that they undermine the already meager SI effect produced by water.

Comparing the different types of surfactants, we find that the most important of these interfacial properties is the CA. In other words, the most important action of the surfactant is it to alter the wettability of the rock from the initial oil-wet state ($\theta = 117.0^\circ$) to the water-wet state (where $\theta < 75^\circ$). The reduction in performance from strong (anionic) to weak (zwitterionic/cationic) is thus correlated with the value of the CA (Fig. 3). It can be therefore concluded that the primary factor controlling the amount of tight oil displaced using SI is the ability of the surfactant to change the wettability of the rock from oil-wet to water-wet. In other words, only if a water-wet state can be realized ($\theta < 75^\circ$) can a sufficiently large capillary pressure be generated that is capable of driving the SI process. Moreover, the more water-wet the surface becomes, the greater the capillary pressure, and the better the efficacy of the SI process. Regarding the impact of IFT, note that the single-component surfactants all produce rather similar IFTs. Therefore, the importance of IFT may only become apparent after an analysis is made of the performance achieved using surfactants with ultra-low IFTs.

The wettability alteration produced by different surfactants may be rationalized by considering the mechanism driving their adsorption to the sandstone surface (Hou et al., 2015). The surface of oil-wet sandstone is negatively charged, so anionic surfactants are more inclined to be adsorbed to the surface through the hydrophobic interaction that occurs between their carbon chains and crude oil components adsorbed on the rock's surface. This leaves their hydrophilic anionic heads exposed, effectively changing the rock from oil-wet to water-wet. Non-ionic surfactants are also believed to be adsorbed to the rock's surface through the interaction between their hydrophobic carbon chains and crude oil components on the rock's surface. This leaves their hydrophilic EO or PO chains exposed outwards, thus changing the rock from oil-wet to water-wet. Cationic/zwitterionic surfactants are believed to be adsorbed to the rock surface by means of ion pairs. As a result, their hydrophobic chains are outwardly exposed, reducing their ability to

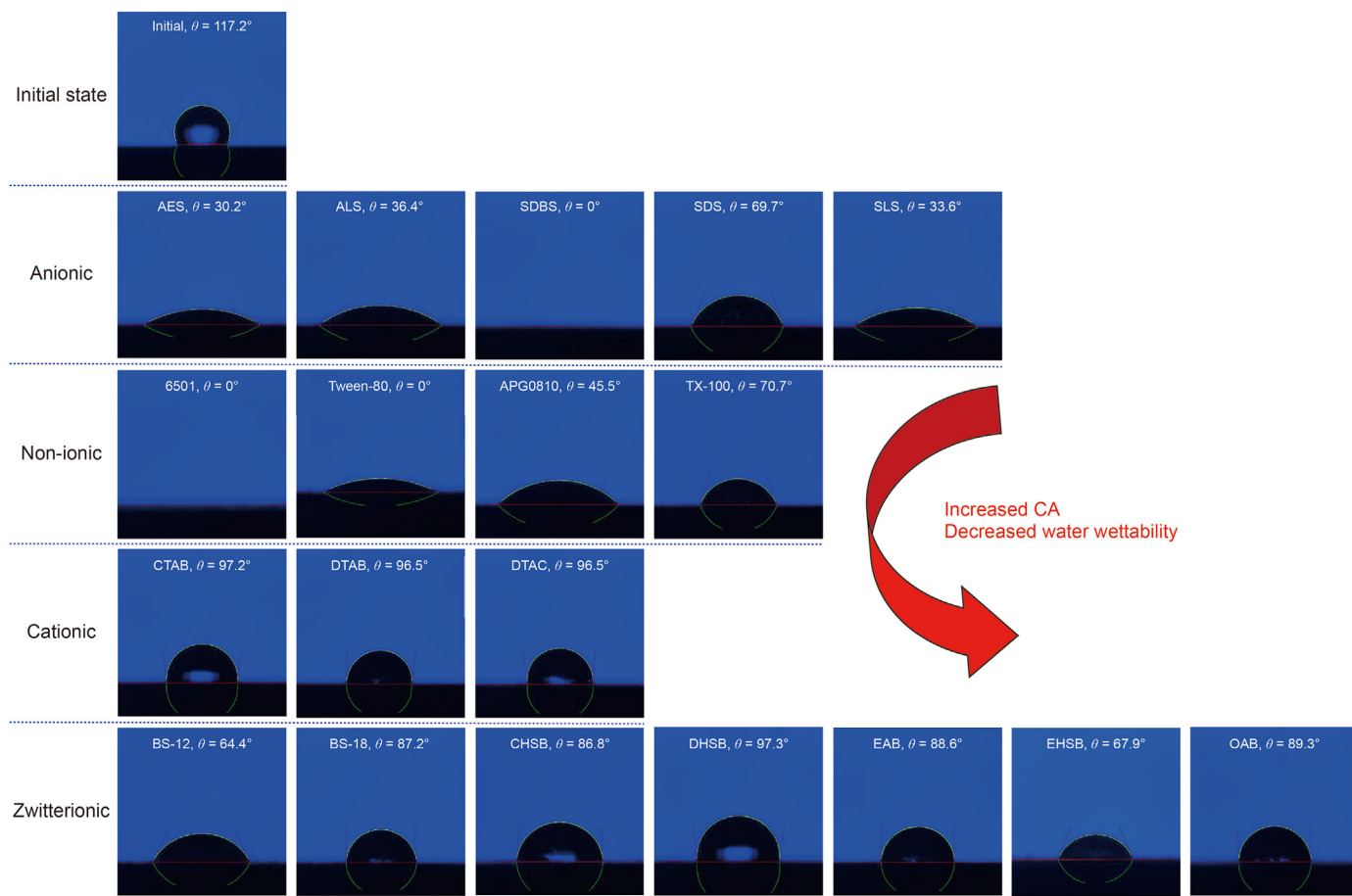


Fig. 3. CAs measured using cores in their initial and surfactant-soaked states.

change the wettability from oil-wet to water-wet. However, the analysis above is only an inference based on the monolayer adsorption model of surfactant, there is still a possibility of multi-layer adsorption of surfactant on the rock (depending on surfactant type, concentration, et al.), and to accurately judge the wettability-alternation mechanism of different surfactants further experimental evidence are needed in the future.

3.1.2. Interfacial properties of surfactant mixtures and their SI efficiency

In light of the above results, two of the most effective single surfactants AES and SDBS (with SI recovery rates of 27.6% and 25.2%, respectively) were combined with other surfactants to see if this had an effect on their ability to discharge crude oil. At the same time, some commercially-available SI products were also collected for comparison. The results are shown in Table 1 and Figs. 4 and 5.

The 16 combined systems all performed better than water. The eight AES-based systems achieved recovery rates of 12.8%–38.5%—the best-performing system being AES:EHSB (1:1). This system yielded IFT and CA values of 0.62 mN/m and 37.7°, respectively. It may be because that the AES assists the wettability alternation (by the hydrophobic adsorption) and EHSB helps in IFT reduction (by the shield of electrostatic repulsion) (Hou et al., 2015), thus, more appropriate IFT and CA is realized. In contrast, the worst-performing system AES:EHSB:6501 (1:1:1), which could only displace 12.8% of the tight oil, yielded an ultra-low IFT value of 0.005 mN/m and a CA value of 70.6°. On the one hand, it seems that using a combination of surfactants can indeed produce a more

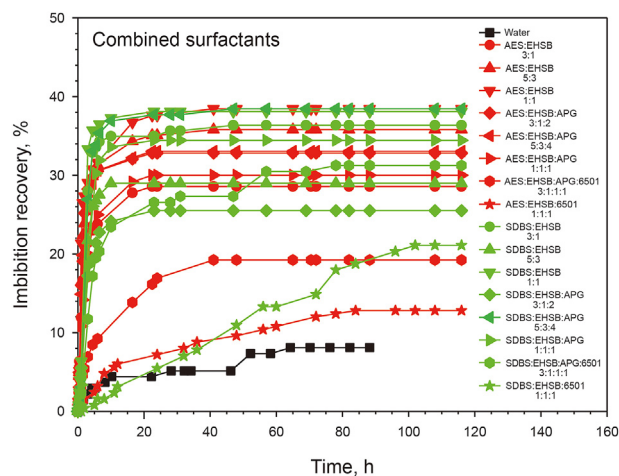


Fig. 4. SI recovery rates obtained using various combinations of different surfactants.

efficient SI system. On the other hand, the comparison given above (AES:EHSB vs. AES:EHSB:6501) suggests that an ultra-low IFT does not seem particularly advantageous when it comes to tight oil SI. Rather, it is (once again) the ability to produce a more strongly hydrophilic surface (smaller CA value) that dominates the displacement effect. This finding differs from the traditional view which suggests ultra-low IFT is highly beneficial (Dou et al., 2021; Guo et al., 2020; Jia et al., 2022; Xiao et al., 2022; Zhao et al., 2022)

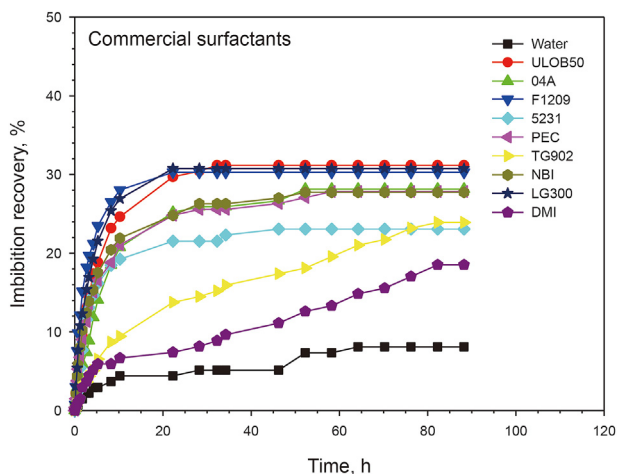


Fig. 5. SI recovery rates obtained using various commercial surfactants.

and lends further support to the importance of wettability regulation. Similar results, which further support the comments made above, were found using SDBS-based mixed systems. The best recovery rate (38.5%) was obtained using the SDBS:EHSB:APG (5:3:4) system ($\sigma = 0.11$ mN/m; $\theta = 31.8^\circ$), whilst the worst (21.1%) was obtained using the SDBS:EHSB:6501 (1:1:1) system ($\sigma = 0.001$ mN/m; $\theta = 56.5^\circ$). Once again, the worst performance was produced by the ultra-low-IFT surfactant and the best by the one with the smallest CA. However, we also cannot say that the higher the IFT, the better. This is because the greater the IFT value, the larger the adhesion work involved, and the more difficult it is to ‘peel’ the oil off the surface. Consider, for example, the combined systems AES:EHSB (3:1) and AES:EHSB:APG:6501 (3:1:1:1). The former has the better performance (28.6% oil recovery) and is characterized by $\sigma = 1.79$ mN/m and $\theta = 24.7^\circ$, compared to the latter (19.2% oil recovery) which is characterized by $\sigma = 1.24$ mN/m and $\theta = 33.8^\circ$. These IFT values are relatively large in the current context but their performances in recovering oil are relatively low. (In this case, note that their performance relative to each other once again appears to simply correlate with their CA values.) Overall, for efficient surfactant-enhanced, SI-mediated recovery of tight oil, the surfactant system needs to have an appropriate IFT (not too high or too low as these scenarios are not necessarily better). The details of what surfactant properties are required for efficient SI of tight oil will be discussed and summarized later on in this paper after we have considered the rest of the SI recovery results.

Our investigation has so far shown that it is feasible to combine anionic surfactants with other types to enhance their SI performance. This research has thus obtained two high-performing systems which can be used in our subsequent studies: AES:EHSB (1:1) and SDBS:EHSB:APG (5:3:4). The SI of tight oil has attracted much attention and some commercial oilfield service companies have also responded by developing various SI agents. Nine commercial systems were therefore collected to compare their performances with the ones prepared by us. The results are shown in Fig. 5.

The IFTs of the commercial systems are generally very low (in the magnitude range 10^{-3} – 10^{-1} mN/m) and, more importantly, they all strongly affect the wettability of the cores from oil-wet to strongly water-wet (with CAs in the range 15.1° – 34.8°). As a result, they generally achieve SI recovery rates (18.5%–31.2%) that exceed those of the single-component surfactants shown in Fig. 2. However, none of them were able to outperform our best systems AES:EHSB (1:1) and SDBS:EHSB:APG (5:3:4) (which both recovered 38.5% of the oil). This proves, once again, that the idea of combining anionic surfactants with zwitterionic and non-ionic surfactants to

develop SI agents for tight oil recovery is a good one. Moreover, 5231 and TG902 (with ultra-low IFT values of 0.0068 and 0.0017 mN/m, respectively) were found to achieve lower SI recovery rates (23.1% and 23.9%, respectively) than those of other systems with much larger IFTs. Once again, this illustrates that ultra-low IFTs are not necessary for SI-enhanced tight oil recovery, and may even have a negative effect.

3.2. Surfactant requirements for the effective SI of tight oil

The results of our experiments have identified some highly efficient surfactants for displacing tight oil via SI. Unfortunately, due to the selectivity of the surfactants to the oil and rock involved, these systems may not be very efficient when different crude oil or rock conditions are involved. Only by clarifying the effect of IFT and CA on SI recovery can we develop better ways of guiding the choice of surfactant to use. In other words, what are the requirements of the surfactant in order for it to be a highly efficient SI agent?

If we assume that the SI recovery rate can be treated as a function of IFT and CA, then the results obtained above for different surfactants can be mapped out in the form of a distribution function. At the same time, as these results were obtained using 0.5-mD cores, further experiments could be conducted using cores with different permeabilities and those results were used to plot similar distributions. In this work, cores with permeabilities of 0.05 and 5.0 mD were also used (Table 2). The distribution functions thus obtained using the different cores are shown in Fig. 6.

Fig. 6(a) shows the results obtained using 0.05-mD cores. As can be seen, the region with the highest level of SI recovery is located mainly in the upper left of the figure, where the IFT is about 10° mN/m and $\theta < 40^\circ$. This is typified by the case of AES ($\sigma = 2.07$ mN/m and $\theta = 30.2^\circ$, giving an SI recovery of 32.0%). Moreover, the SI recovery rate decreases significantly as IFT decreases and CA increases and we move towards the lower right part of the chart. For example, the surfactant EHSB appears in this region ($\sigma = 0.07$ mN/m; $\theta = 67.9^\circ$; SI recovery rate 3.3%). This shows that in order to achieve efficient SI in 0.05-mD cores, an appropriate IFT level is $\sim 10^\circ$ mN/m (and lower values are not better) and the wettability should correspond to $\theta < 40^\circ$. Curves corresponding to $N_B^{-1} = 5$ and $N_B^{-1} = 0.2$ were further added to this figure. The region with highest level of IS recovery lies far to the left of the $N_B^{-1} = 5$ curve, indicating that capillary pressure is the key force driving the SI process (Schechter et al., 1991; Høgnesen et al., 2004). This explains why efficient SI requires 10° mN/m and $\theta < 40^\circ$ (low IFT values and high CA values reduce the capillary force).

The distribution obtained using the 0.5-mD cores is shown in Fig. 6(b). Compared to the previous distribution, the high-SI recovery region in this case is slightly further to the right and slightly

Table 2 Interfacial properties of the surfactants used and corresponding SI recovery rates measured in cores with permeabilities of 0.05, 0.5, and 5.0 mD.

No.	SI fluids	IFT, mN/m	CA, °	SI recovery, %			
				0.05 mD	0.5 mD	5.0 mD	
1	Water	20.30	89.0	15.7	8.1	28.9	
2	Anionic	AES	2.07	30.2	32.0	27.6	31.7
3		ALS	1.74	36.4	21.2	22.5	34.8
5		SDBS	0.64	0.0	28.2	25.2	30.1
7	Cationic	CTAB	0.10	97.2	1.6	0.8	17.3
9		DTAC	0.70	96.5	0.8	0.0	11.6
11	Zwitterionic	BS-18	0.20	87.2	1.6	0.4	20.1
15		EHSB	0.07	67.9	3.3	2.4	25.8
16		OAB	0.21	89.3	0.7	0.4	18.1
17	Non-ionic	6501	0.21	0.0	14.8	19.6	15.9
19		APG0810	0.47	45.5	22.6	20.0	32.5
20		TX-100	0.48	70.7	25.2	18.4	35.5

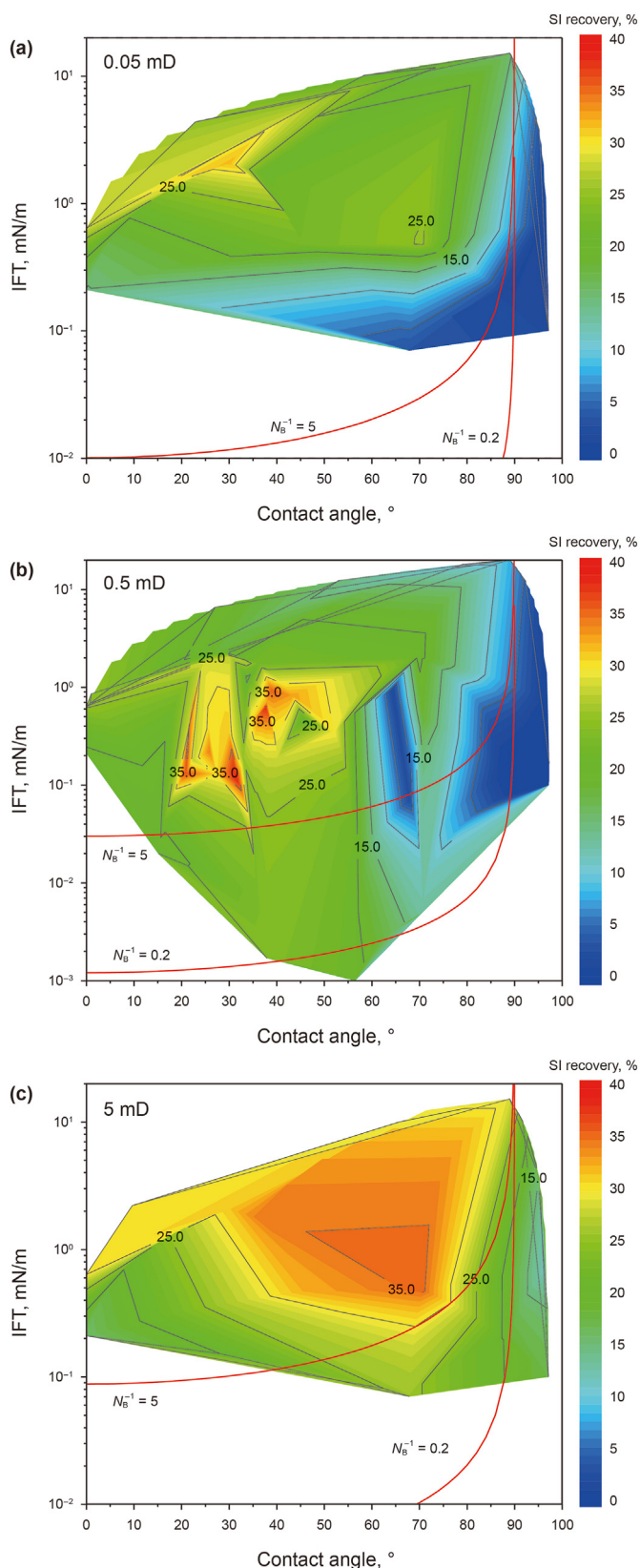


Fig. 6. SI recovery rates plotted as functions of IFT and CA for cores with permeabilities of 0.05 (a), 0.5 (b), and 5.0 (c) mD.

lower down. The optimum IFT is therefore in the range of 10^{-1} – 10^0 mN/m and we also need $\theta < 55^\circ$. Surfactants with these properties are therefore more likely to work well in removing tight

oil via IS. It is noteworthy that the two optimal systems we developed both lie in this region (AES:EHSB (1:1) has $\sigma = 0.62$ mN/m and $\theta = 37.7^\circ$; SDBS:EHSB:APG (5:3:4) has $\sigma = 0.11$ mN/m and $\theta = 31.8^\circ$ —both yielding an SI recovery rate of 38.5%. As before, the closer one moves to the lower right of the figure, the lower the SI recovery rate (e.g. CHSB has $\sigma = 0.12$ mN/m, $\theta = 86.8^\circ$, and SI recovery of 0.4%; AES:EHSB:6501 (1:1:1) has $\sigma = 0.005$ mN/m, $\theta = 70.6^\circ$, and SI recovery of 12.8%). Overall, the region with the highest IS recovery rate moves closer to the $N_b^{-1} = 5$ curve but remains to the left of it, indicating that capillary pressure again plays a key role in the SI process when the permeability of the core is 0.5 mD.

Further increasing the permeability to 5.0 mD, the results are obtained as shown in Fig. 6(c). It is clear from this diagram that the region with high-SI recovery is significantly larger than in the previous diagrams (due to the increased permeability). The optimum region corresponds to IFT values in the range of 10^{-1} – 10^0 mN/m and $\theta < 70^\circ$. Moreover, this area clearly lies further to the right than in the previous diagrams. This reflects a weakening of one of the requirements for efficient SI: that CA be reduced to favorably regulate the wettability of the core. Take, for example, TX-100. This surfactant has a relatively large CA value of 70.7° (close to the bound value of 70.0°) and an IFT value of 0.48 mN/m but it still manages to achieve an excellent SI recovery rate of 35.5% in these high-permeability cores. Note also that the high-SI recovery region is closer still to the $N_b^{-1} = 5$ curve (compared to the 0.05 and 0.5 mD cases). However, it is still distributed to the left of the curve, showing that the capillary force remains the key driver of the SI process despite an increase in the effect of buoyancy.

To summarize: cores with different permeabilities impose different requirements on the surfactant if efficient SI is to be achieved. Cores with permeabilities of 0.05, 0.5, and 5.0 mD require surfactants with IFT and CA values of 10^0 mN/m, $< 40^\circ$; 10^{-1} – 10^0 mN/m, $< 55^\circ$; and 10^{-1} – 10^0 mN/m, $< 70^\circ$, respectively. Thus, when the permeability decreases, we need to increase the IFT and decrease the CA of the surfactant in order to increase capillary pressure and achieve efficient SI.

3.3. Activation depth of the tight oil

In the above experiments, the SI recovery of tight oil was evaluated but the results give no indication of the depth to which the SI process can exhaust the crude oil present in the core. That is, we need to know to what depth the crude oil can be removed from the matrix using the SI effect when the surfactant solution only flows in natural fractures and those generated via hydraulic fracturing. Additional SI tests were therefore implemented using larger cores ($5.0 \text{ cm} \times 5.0 \text{ cm} \times 5.0 \text{ cm}$) and a wider range of permeabilities (0.005–30.0 mD). More importantly, the distribution of the residual oil remaining in the cores was determined by scanning the cores using the CT technique. This approach gives us the opportunity to directly observe the way the tight oil is mobilized by the surfactant-mediated SI process.

3.3.1. Effect of permeability

The optimized AES:EHSB (1:1) system ($\sigma = 0.62$ mN/m; $\theta = 37.7^\circ$) was used for these tests as it achieved an excellent SI recovery rate of 38.5% in the 0.5-mD cores. The surfactant was used to displace tight oil from large, cubic cores with permeabilities of 0.005, 0.1, and 30.0 mD, giving the results shown in Figs. 7 and 8.

Fig. 7 shows that the oil recovery rate from the larger cubic cores is strongly dependent on the permeability of the core (5.6%, 7.8%, and 30.6% of the oil could be recovered from cores with permeabilities of 0.005, 0.1, and 30.0 mD, respectively). In cores with

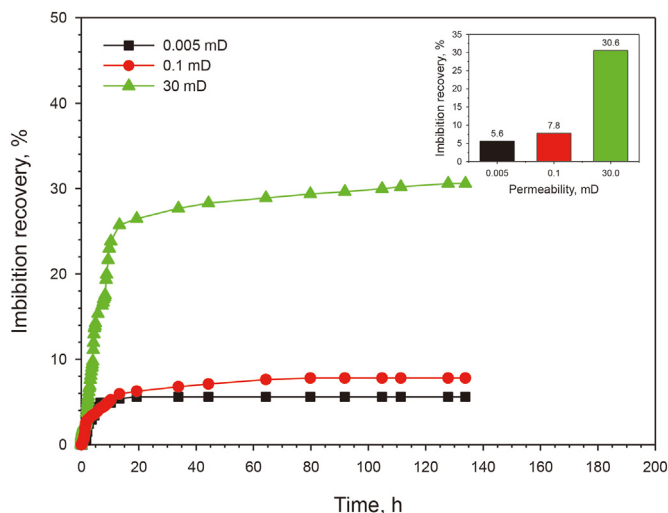


Fig. 7. SI recovery of oil from large, cubic cores with different permeabilities. The surfactant AES:EHSB (1:1) was used in each case ($\sigma = 0.62$ mN/m).

permeabilities in the range of 0.005–0.1 mD, less than 10% of the crude oil could be extracted (highlighting the great difficulty encountered when developing tight oil reservoirs). Note that these

SI recovery rates (obtained using cores of 5.0 cm × 5.0 cm × 5.0 cm) are all significantly lower than that previously obtained using the same surfactant to displace oil from a smaller cylindrical core ($\phi 2.5$ cm × 3.0 cm and 0.5 mD permeability, yielding an SI recovery rate of 38.5%). Increasing the core size therefore leads to a significant deterioration of the SI effect. The reason for this may be because the mobilization depth of the tight oil by the SI process is limited and roughly constant (as a result, the larger the core size, the smaller the macroscopic SI recovery rate). This can be verified by visualizing the mobilization depth (Fig. 8).

Fig. 8 shows the distribution of the invasive water (red) as it enters cores initially saturated with oil (blue). As SI proceeds, the areas where the water can invade gradually change to yellow and then red. The penetration depth of the invading water/surfactant and the starting distribution of the crude oil can therefore be ascertained according to the observed change in color. As can be seen, the SI recovery rates are very low in the low-permeability cores. Thus, the 0.005-mD core only gave up 0.5% and 5.5% of its oil after soaking for 1.5 and 134.0 h, respectively. Over the same time periods, the 0.1-mD core gave up 2.5% and 7.8%, respectively. More importantly, in these cores, only the outermost few millimeters of the core changed color from blue to yellow/red. This shows that it was very difficult for the surfactant solution to enter deep into the core via SI. It also shows that the mobilization depth

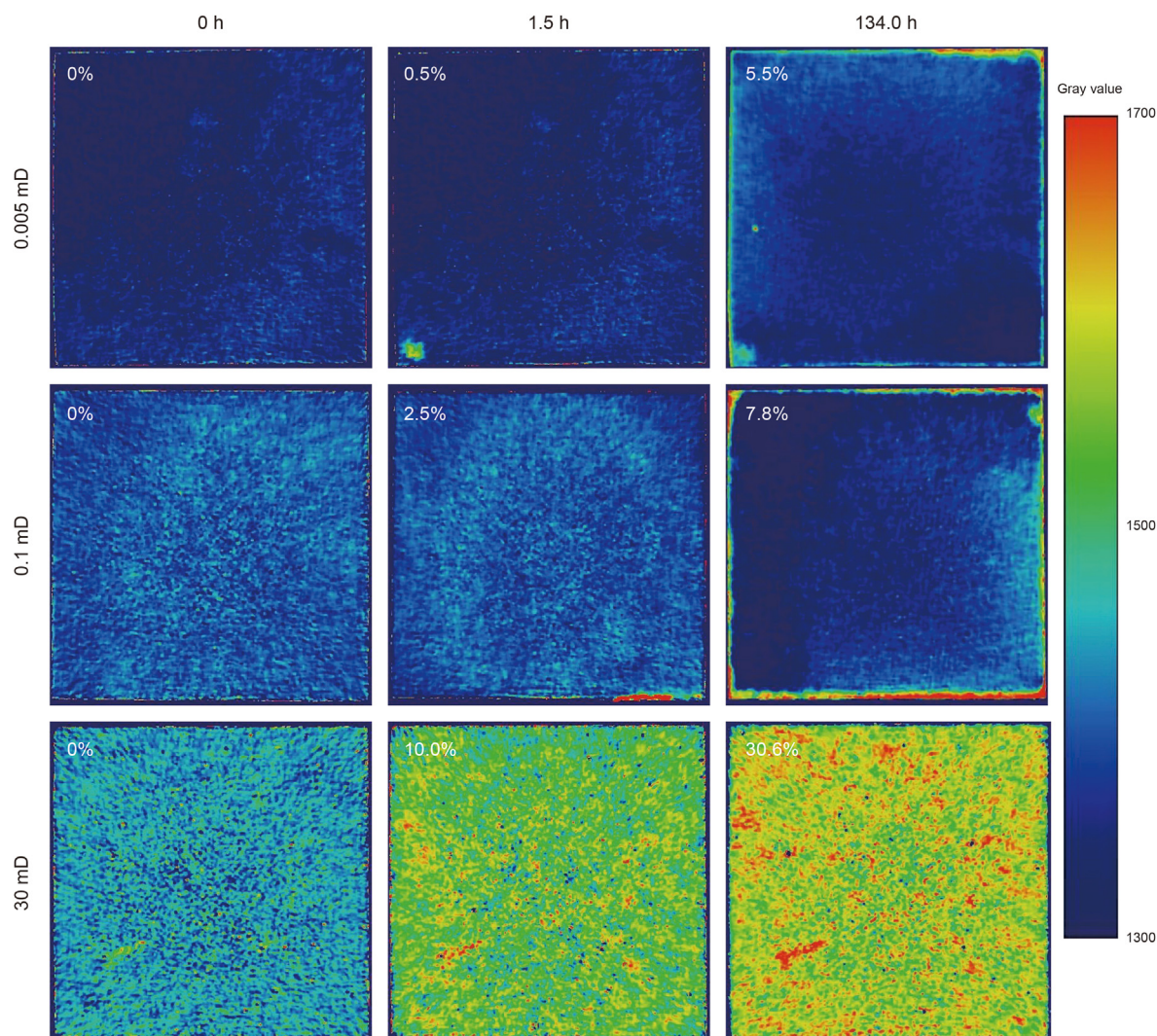


Fig. 8. CT scanning results showing the distribution of invasive water (red) and residual oil (blue) during the imbibition of a solution of AES:EHSB (1:1) surfactant ($\sigma = 0.62$ mN/m).

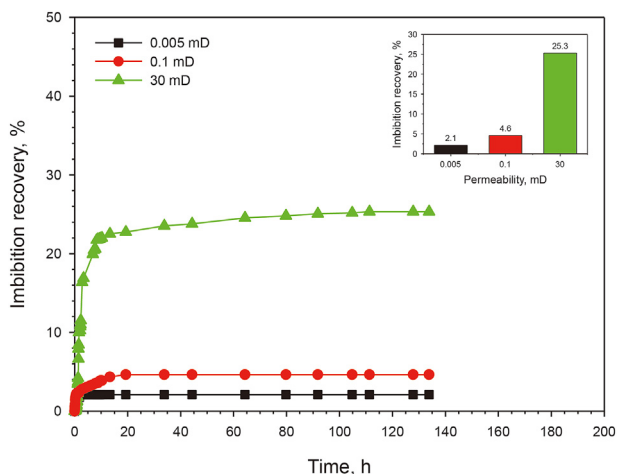


Fig. 9. Oil recovery rate from large, cubic cores using TG902 ($\sigma = 1.7 \times 10^{-3}$ mN/m).

of the crude oil is only a few millimeters. So, the suggestion that tight oil can be extracted via the well-known SI effect is not as convincing as traditionally imagined. Increasing the size of the core (from $\phi 2.5$ cm \times 3.0 cm to 5.0 cm \times 5.0 cm \times 5.0 cm, for example) will lead to a decrease in surface area per unit volume (and hence

recovery rate of oil stored). This explains why there is subsequently a significant decrease in the SI recovery rate achieved using the AES:EHSB (1:1) system (from 38.5% in Figs. 4 to 5.5%/7.8% in Fig. 7). Accordingly, it can be also speculated that the lower the fracture density, the larger the corresponding matrix size, and so the worse the SI-mediated oil extraction effect. Conversely, of course, a higher fracture density will lead to a much better extraction effect.

The limited activation depth of tight oil may arise for several reasons. Two possibilities are as follows: (i) Different capillary forces are formed in small and large pores. This difference is the key to SI as it enables water to enter small pores and displace crude oil into large ones and then be recovered. However, the pore structure of tight rock is extremely complex and the diameters of the pores are highly changeable. When the oil–water interface pushes into the rock and encounters relatively large pores, the capillary pressure difference can disappear and imbibition will stop. As a result, the water will not continue to push deeper into the rock. (ii) The pores of tight oil are very small (sub-micron–nanometer level). Therefore, the liquid layer bound to the surface of the pores will strongly inhibit the flow of liquid inside them. As a result, a ‘start-up’ pressure is known to exist in such pores (An et al., 2019; Wensink et al., 2015). When the pressure difference of the capillary is less than this start-up pressure, water cannot enter the tight matrix and, therefore, will not be able to displace the oil therein.

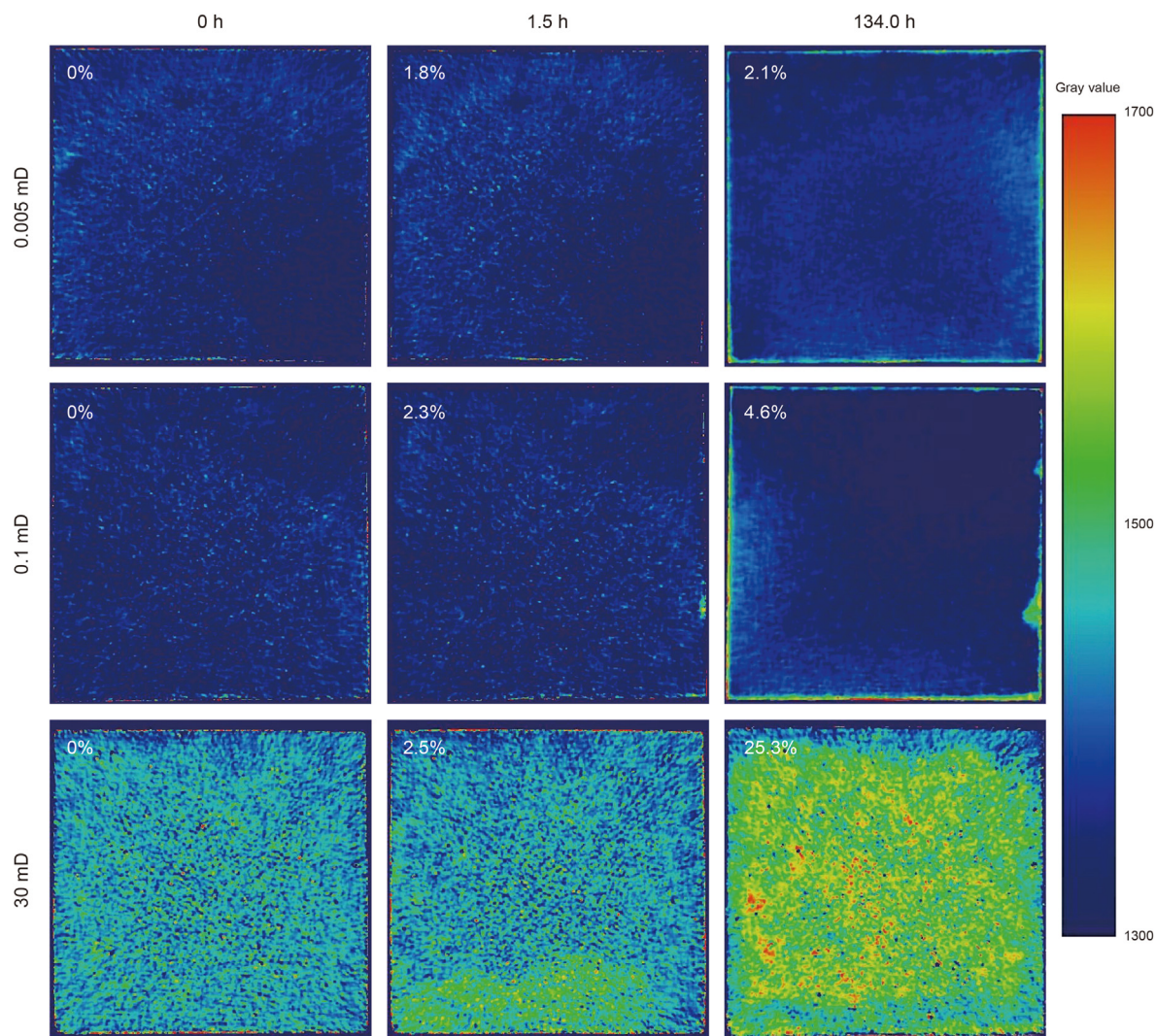


Fig. 10. CT results showing the distribution of invasive water (red) and residual oil (blue) during the imbibition of TG902 ($\sigma = 1.7 \times 10^{-3}$ mN/m).

When the permeability was increased to 30.0 mD, the SI recovery rate increased significantly, reaching 30.6% (traditionally, such a core corresponds to what is classified as a ‘low-permeability reservoir’). In this case, the color of the whole core was converted to yellow or red, indicating that the water was able to enter the whole of the core via the SI effect (and that the starting depth of the crude oil was at least a few centimeters). Thus, SI would be highly effective in conventional low-permeability reservoirs (i.e. 30 mD). However, it would, perhaps, not be very effective in tight oil reservoirs (i.e. 0.005 and 0.1 mD).

3.3.2. Effect of IFT

Another surfactant, TG902, was also selected to perform water–oil distribution tests (Figs. 9 and 10). This agent was chosen because of its ultra-low IFT value (0.0017 mN/m), which is much smaller than that of the AES:EHSB (1:1) system (0.62 mN/m). By comparing the two sets of results, the impact that IFT has on SI recovery and crude oil mobilization could be further investigated.

Fig. 9 shows that the TG902 solution removed less of the oil from the cores than the AES:EHSB system even though it has a much smaller IFT value (0.0017 mN/m vs. 0.62 mN/m). More specifically, after 134 h, only 2.1%, 4.6%, and 25.3% of the oil could be removed from the 0.005-, 0.1-, and 30-mD cores, respectively. This poorer performance may be because the lower IFT value results in a lower capillary pressure and hence weaker SI effect (as the key force driving SI in the cores has proved to be capillary pressure, see Fig. 6). Therefore, in the permeability range adopted in these experiments (0.005–30.0 mD), an ultra-low IFT appears to impair the SI process and inhibit the mobilization of crude oil.

However, we cannot generally say that an ultra-low IFT is unfavorable to the SI process as the effect of IFT on SI recovery also depends on permeability (as can be seen from Fig. 9). As a test, our imbibition results were further supplemented by conducting experiments using cores with permeabilities of 60 mD. It was found that the SI recovery rate achieved using the AES:EHSB system was only 12.6% (which was much less than that using a 30 mD core), while the TG902 system displaced a significant recovery rate of the oil: 38.5%. This is presumably because the influence of capillary force on SI is weakened in high-permeability cores, while the effect of buoyancy is enhanced (see, for example, Fig. 6 which shows that the higher the permeability, the weaker the influence of capillary force and the stronger the influence of buoyancy). As a result, the TG902 with its ultra-low IFT is able to achieve the SI-mediated extraction of crude oil via the buoyancy effect. Thus, ultra-low IFT can be advantageous when the permeability is relatively high.

The distribution of invasive TG902 solution and residual oil during SI is shown in Fig. 10. The TG902 was able to achieve an intrusion depth of several millimeters in the 0.005- and 0.1-mD cores but fully enter and spread throughout the higher (30 mD) permeability core. These results are therefore very similar to those obtained using the AES:EHSB system. This once again shows that surfactant solutions have very limited initiation depths in tight oil cores (i.e. 0.005 and 0.1 mD) and essentially ideal invasive effects in cores that are more permeable (e.g. 30 mD).

3.4. Mobilization of oil from pores of different sizes

Cores with different permeabilities were scanned using an NMR scanner, before and after the imbibition of AES:EHSB (1:1), to investigate the sizes of the pores from which the oil was recovered. Fig. 11 shows the results obtained. In these graphs, the amplitude of the T_2 signal represents the strength of the hydrogen signal (which essentially reflects the level of oil saturation in those pores). The value of T_2 itself reflects the size of the pores involved (smaller T_2 values correspond to smaller pores).

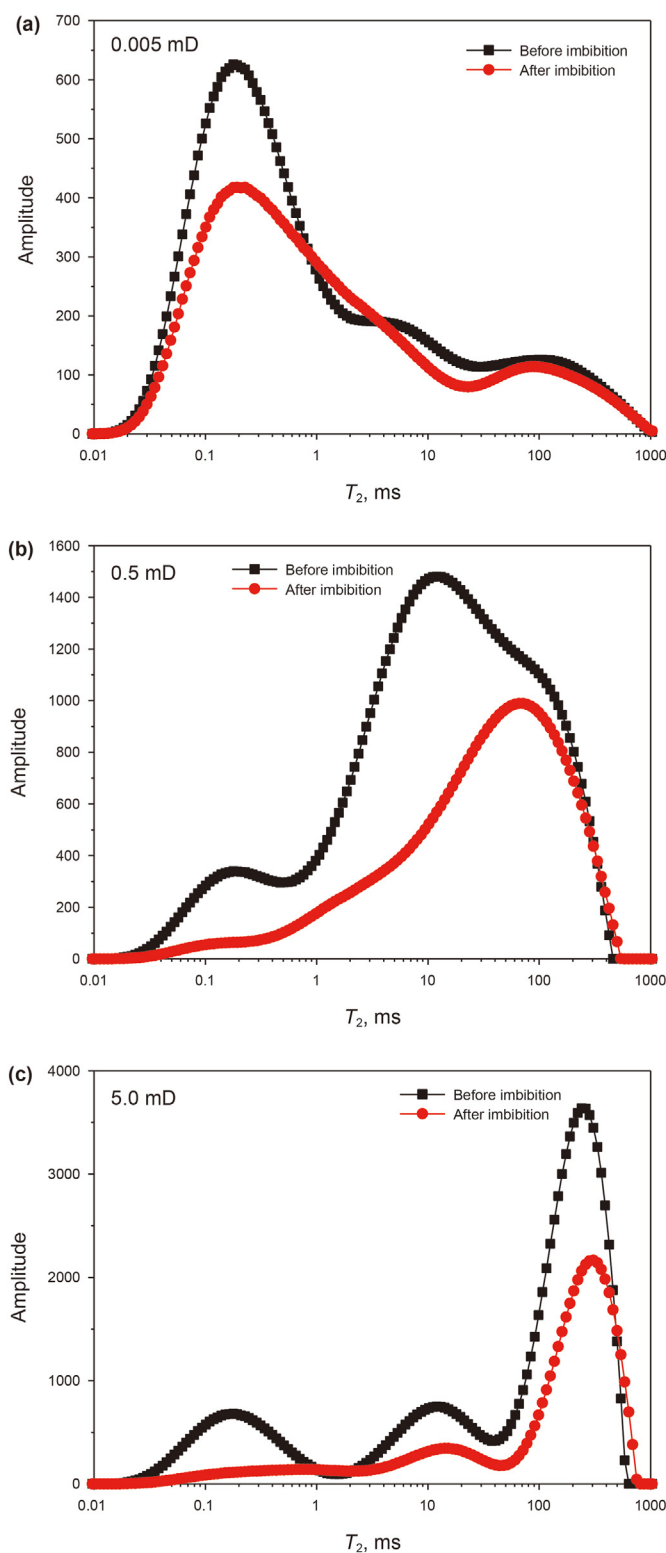


Fig. 11. Mobilization of oil from pores of different sizes. The graphs show the NMR (T_2) relaxation time scans recorded before and after the cores were subjected to SI using AES:EHSB (1:1) ($\sigma = 0.62$ mN/m). The results correspond to cores with permeabilities of 0.005 (a), 0.5 (b), and 5.0 (c) mD.

Fig. 11 shows that the lower the permeability of the core, the greater the proportion of small pores present (corresponding to T_2 values of 0.01–1 ms). In particular, Fig. 11(a) shows that the low-permeability core (0.005 mD) contains a large proportion of oil in

these small pores. Correspondingly, there is less oil in the medium and large pores (T_2 values in the range 1–1000 ms). However, as the permeability increases to 0.5 mD (Fig. 11(b)) and 5.0 mD (Fig. 11(c)), the amplitudes of the signals coming from these medium–large pores increase and eventually dominate.

If we now compare the T_2 signals before and after the SI process, how much oil is mobilized from the pores of different sizes can be judged. In Fig. 11(a) (0.005-mD core), the amplitude of the signal from the oil in the small pores (T_2 range 0.01–1 ms) is significantly reduced after imbibition, while that from the oil in the medium and large pores (T_2 range 1–1000 ms) just decreases slightly. This shows that the SI process mainly removed the crude oil that is stored inside the small pores in the tight core. In fact, this provides further evidence that the capillary force is the key force driving the SI process. This is because the smaller the pore size, the greater the capillary force: the water will therefore preferentially enter those small pores, resulting in a significant reduction of the T_2 signal from the oil present. As the permeability of the core increases (Fig. 11(b) and (c)), the oil becomes progressively more associated with pores that are larger in size. However, when SI occurs, the T_2 signals show that the oil is removed from pores of all sizes, showing that the crude oil inside them has been activated by the surfactant. Note, however, that the T_2 signal from the oil in the small pores is most significantly affected and is almost reduced to zero by the SI process.

These observations should be compared with the oil mobilization characteristics achieved when the more traditional oil-flooding process is used. This procedure involves directly pumping a fluid (e.g. surfactant solution) into a core to displace the oil there. In this case, the T_2 signal from the oil in the medium and large pores decreases most significantly (while that from the oil in the small pores decreases less significantly) (Wensink et al., 2015; Wei et al., 2020). This is because the fluid is pumped into the core and therefore preferentially flows into the larger pores (where the flow resistance is relatively small). Thus, it is the oil in the large pores that is replaced while the smaller pores are less affected. In other words, the two cases differ because different driving powers are involved in displacing the oil: in traditional flooding, the pump pressure preferentially displaces the crude oil stored in the medium and large pores, while the SI process is driven by capillary force which preferentially removes crude oil from the small pores.

4. Conclusions

This work aimed to deduce the best surfactant(s) required to optimize the SI effect in tight oil reservoirs and determine the nature of the basic surfactant properties required for efficient SI. Our approach was to conduct a large number of surfactant-mediated SI experiments and to analyze the oil distributions in certain cores using CT and NMR scanners. The major conclusions of the work can be summarized as follows.

- (1) The SI performances of different types of surfactants decrease in the order: anionic, non-ionic, cationic, and zwitterionic. By combining surfactants, more efficient systems could be created. Our best agents, AES:EHSB (1:1) and SDBS:EHSB:APG (5:3:4), yielded SI recovery rates of 38.5%, which is significantly better than the oil recovery rate using the commercial surfactants tested.
- (2) The surfactant properties required for efficient SI are dependent on the permeability of the core. Low permeability implies the agent should have larger IFT values and smaller CAs as these regimes increase the capillary pressure which, in turn, increases the efficiency of the SI process. Cores with permeabilities of 0.05, 0.5, and 5.0 mD require as follows:

10^0 mN/m, $< 40^\circ$; 10^{-1} – 10^0 mN/m, $< 55^\circ$; and 10^{-1} – 10^0 mN/m, $< 70^\circ$, respectively.

- (3) The activation depth of tight oil achieved using the best SI-mediated surfactants is just a few millimeters in cores with permeabilities of 0.005 and 0.1 mD. Thus, it is very difficult to displace oil from the corresponding tight reservoirs using SI. With 30.0-mD cores, the surfactant solution is able to enter the whole of the core via the SI effect (so the starting depth of the crude oil is at least a few centimeters). This means that SI is an effective (and hence highly worthwhile) approach to developing conventional low-permeability reservoirs.
- (4) As it is primarily driven by capillary pressure, SI preferentially removes crude oil from the small pores in the core. On the other hand, the traditional flooding process is driven by the pump-induced flow of the injected fluid and therefore preferentially displaces the crude oil stored in the medium and large pores.

CRediT authorship contribution statement

Ming-Chen Ding: Writing – original draft, Conceptualization. **Xin-Fang Xue:** Resources. **Ye-Fei Wang:** Supervision, Funding acquisition. **Chu-Han Zhang:** Investigation. **Shi-Ze Qiu:** Writing – review & editing.

Declaration of competing interest

The authors declared that they have no conflicts of interest to this work.

We declare that we do not have any commercial or associative interest that represents a conflict of interest in connection with the work submitted.

Acknowledgments

The authors thank the National Natural Science Foundation of China (Grant No. 52474071) for their financial support.

References

- Alvarez, J.O., Neog, A., Jais, A., Schechter, D.S., 2014. Impact of surfactants for wettability alteration in stimulation fluids and the potential for surfactant EOR in unconventional liquid reservoirs. In: SPE Unconventional Resources Conference. <https://doi.org/10.2118/169001-MS>.
- Alvarez, J.O., Schechter, D.S., 2017. Wettability alteration and spontaneous imbibition in unconventional liquid reservoirs by surfactant additives. SPE Reservoir Eval. Eng. 20, 107. <https://doi.org/10.2118/177057-PA>.
- An, W.Q., 2019. Study on Key Scientific Problems of Percolation and Oil Displacement in Tight Low Permeability Reservoirs. Ph.D Dissertation. China University of Petroleum (Beijing), pp. 56–68.
- Chaudhary, A.S., Ehlij-economides, C.A., Wattenbarger, R., 2011. Shale oil production performance from a stimulated reservoir volume. In: SPE Annual Technical Conference and Exhibition. <https://doi.org/10.2118/147596-MS>.
- Cheng, Z.L., Ning, Z.F., Yu, X.F., Wang, Q., Zhang, W.T., 2019. New insights into spontaneous imbibition in tight oil sandstones with NMR. J. Petrol. Sci. Eng. 179, 455–464. <https://doi.org/10.1016/j.petrol.2019.04.084>.
- Dai, C.L., Cheng, R., Sun, X., Liu, Y.F., Zhou, H.D., Wu, Y.N., You, Q., Zhang, Y., Sun, Y.P., 2019. Oil migration in nanometer to micrometer sized pores of tight oil sandstone during dynamic surfactant imbibition with online NMR. Fuel 245, 544–553. <https://doi.org/10.1016/j.fuel.2019.01.021>.
- Dou, L.B., Xiao, Y.J., Gao, H., Wang, R., Liu, C.L., Sun, H.B., 2021. The study of enhanced displacement efficiency in tight sandstone from the combination of spontaneous and dynamic imbibition. J. Petrol. Sci. Eng. 199, 108327. <https://doi.org/10.1016/j.petrol.2020.108327>.
- Fragoso, A., Selvan, K., Aguilera, R., 2018. Breaking a paradigm: can oil recovery from shales be larger than oil recovery from conventional reservoirs? The answer is Yes. In: SPE Canada Unconventional Resources Conference. <https://doi.org/10.2118/189784-MS>.
- Gu, X.Y., Pu, C.S., Huang, H., Huang, F.F., Li, Y.J., Liu, Y., Liu, H.C., 2017. Micro-influencing mechanism of permeability on spontaneous imbibition recovery for tight sandstone reservoirs. Petrol. Explor. Dev. 44 (6), 1003–1009. <https://doi.org/10.1016/j.petrol.2017.06.003>.

- [doi.org/10.1016/S1876-3804\(17\)30112-X](https://doi.org/10.1016/S1876-3804(17)30112-X).
- Guo, J.C., Li, M., Chen, C., Tao, L., Liu, Z., Zhou, D.S., 2020. Experimental investigation of spontaneous imbibition in tight sandstone reservoirs. *J. Petrol. Sci. Eng.* 193, 107395. <https://doi.org/10.1016/j.petrol.2020.107395>.
- Høgnesen, E.J., Standnes, D.C., Austad, T., 2004. Scaling spontaneous imbibition of aqueous surfactant solution into preferential oil-wet carbonates. *Energy & Fuels* 18 (6), 1665–1675. <https://doi.org/10.1021/ef040035a>.
- Hou, B.F., Wang, Y.F., Huang, Y., 2015. Mechanistic study of wettability alteration of oil-wet sandstone surface using different surfactants. *Appl. Surf. Sci.* 330, 56–64. <https://doi.org/10.1016/j.apsusc.2014.12.185>.
- Jia, C.Z., Zou, C.N., Li, J.Z., Li, D.H., Zheng, M., 2012. Assessment criteria, main types, basic features and resource prospect of the tight oil in China. *Acta Pet. Sin.* 33 (3), 343–350. <https://doi.org/10.7623/syxb201203001> (in Chinese).
- Jia, R.X., Kang, W.L., Li, Z., Yang, H.B., Gao, Z.D., Zheng, Z.W., 2022. Ultra-low interfacial tension (IFT) zwitterionic surfactant for imbibition enhanced oil recovery (IEOR) in tight reservoirs. *J. Mol. Liq.* 368, 120734. <https://doi.org/10.1016/j.molliq.2022.120734>.
- Jiang, Z.H., Li, G.R., Zhao, P.Q., Zhou, Y., Mao, Z.Q., Liu, Z.D., 2023. Study on spontaneous imbibition and displacement characteristics of mixed-wet tight sandstone reservoir based on high-precision balance and NMR method. *Fuel* 345, 128247. <https://doi.org/10.1016/j.fuel.2023.128247>.
- Kiani, M., Hsu, T.P., Roostapour, A., Kazempour, M., Tudor, E., 2019. A novel enhanced oil recovery approach to water flooding in saskatchewan's tight oil plays. In: *Unconventional Resources Technology Conference*. <https://doi.org/10.15530/urtec-2019-419>.
- Liu, C., Wang, T.R., You, Q., Du, Y.C., Zhao, G.Z., Dai, C.L., 2024. The effects of various factors on spontaneous imbibition in tight oil reservoirs. *Petrol. Sci.* 21, 315–326. <https://doi.org/10.1016/j.petsci.2023.09.022>.
- Liu, J.R., Sheng, J.J., 2019. Experimental investigation of surfactant enhanced spontaneous imbibition in Chinese shale oil reservoirs using NMR tests. *J. Ind. Eng. Chem.* 72, 414–422. <https://doi.org/10.1016/j.jiec.2018.12.044>.
- Neog, A., Schechter, D.S., 2016. Investigation of surfactant induced wettability alteration in Wolfcamp Shale for hydraulic fracturing and EOR applications. In: *SPE Improved Oil Recovery Conference*. <https://doi.org/10.2118/179600-MS>.
- Qi, S.C., Yu, H.Y., Han, X.B., Xu, H., Liang, T.B., Jin, X., Qu, X.F., Du, Y.J., Xu, K., 2023. Countercurrent imbibition in low-permeability porous media: non diffusive behavior and implications in tight oil recovery. *Petrol. Sci.* 20, 322–336. <https://doi.org/10.1016/j.petsci.2022.10.022>.
- Ren, W.D., Ma, C., Huang, X.Y., Gu, W., Chen, Y., Liu, X.Y., 2023. Dynamic and static imbibition characteristics of tight sandstone based on NMR. *Geoenergy Science and Engineering* 229, 212052. <https://doi.org/10.1016/j.geoen.2023.212052>.
- Schechter, D.S., Zhou, D.Q., Orr, F.M., 1991. Capillary imbibition and gravity segregation in low IFT systems. In: *66th Annual Technical Conference and Exhibition of the Society of Petroleum Engineers*. <https://doi.org/10.2118/22594-MS>.
- Sheng, J.J., 2015. Enhanced oil recovery in shale reservoirs by gas injection. *J. Nat. Gas Sci. Eng.* 22 (1), 252–259. <https://doi.org/10.1016/j.jngse.2014.12.002>.
- Sheng, J.J., 2017. What type of surfactants should be used to enhance spontaneous imbibition in shale and tight reservoirs? *J. Petrol. Sci. Eng.* 159, 635–643. <https://doi.org/10.1016/j.petrol.2017.09.071>.
- Shuler, P., Tang, H.X., Lu, Z.Y., Tang, Y.C., 2011. Chemical process for improved oil recovery from Bakken shale. In: *Canadian Unconventional Resources Conference*. <https://doi.org/10.2118/147531-MS>.
- Sieminsk, A., Maisonneuve, C., 2013. Status and outlook for shale gas and tight oil development in the US. In: *Houston, TX: Platts-North American Crude Marketing Conference*.
- Tian, W.B., Wu, K.L., Feng, D., Gao, Y.L., Li, J., Chen, Z.X., 2023. Dynamic contact angle effect on water-oil imbibition in tight oil reservoirs. *Energy* 284, 29209. <https://doi.org/10.1016/j.energy.2023.129209>.
- Todd, H.B., Evans, J.G., 2016. Improved oil recovery IOR pilot projects in the Bakken Formation. In: *SPE Low Perm Symposium*. <https://doi.org/10.2118/180270-MS>.
- Wang, D.M., Butler, R., Zhang, J., Seright, R., 2012. Wettability survey in Bakken shale with surfactant-formulation imbibition. *SPE Reservoir Eval. Eng.* 15 (6), 695–705. <https://doi.org/10.2118/153853-PA>.
- Wang, J., Liu, H.Q., Qian, G.B., Peng, Y.C., Gao, Y., 2019. Investigations on spontaneous imbibition and the influencing factors in tight oil reservoirs. *Fuel* 236, 755–768. <https://doi.org/10.1016/j.fuel.2018.09.053>.
- Wei, B., Liu, J., Zhang, X., Xiang, H., Zou, P., Cao, J., Bai, M.X., 2020. Nuclear magnetic resonance (NMR) mapping of remaining oil distribution during sequential rate waterflooding processes for improving oil recovery. *J. Petrol. Sci. Eng.* 190, 107102. <https://doi.org/10.1016/j.petrol.2020.107102>.
- Wei, J.G., Fu, L.Q., Zhao, G.Z., Zhao, X.Q., Liu, X.R., Wang, A.L., Wang, Y., Cao, S., Jin, Y.H., Yang, F.R., Liu, T.Y., Yang, Y., 2023. Nuclear magnetic resonance study on imbibition and stress sensitivity of lamellar shale oil reservoir. *Energy* 282, 128872. <https://doi.org/10.1016/j.energy.2023.128872>.
- Wensink, E.J.W., Hoffmann, A.C., Apol, M.E.F., Berendsen, H.J.C., 2015. Properties of adsorbed water layers and the effect of adsorbed layers on interparticle forces by liquid bridging. *Langmuir* 16 (19), 7392–7400. <https://doi.org/10.1021/la000009e>.
- Xiao, L.X., Hou, J.R., Wen, Y.C., Qu, M., Wang, W.J., Wu, W.P., Liang, T., 2022. Imbibition mechanisms of high temperature resistant microemulsion system in ultra-low permeability and tight reservoirs. *Petrol. Explor. Dev.* 49 (6), 1398–1410. [https://doi.org/10.1016/S1876-3804\(23\)60358-1](https://doi.org/10.1016/S1876-3804(23)60358-1).
- Yang, Z.M., Liu, X.W., Li, H.B., Lei, Q.H., Luo, Y.T., Wang, X.Y., 2019. Analysis on the influencing factors of imbibition and the effect evaluation of imbibition in tight reservoirs. *Petrol. Explor. Dev.* 46 (4), 779–785. [https://doi.org/10.1016/S1876-3804\(19\)60235-1](https://doi.org/10.1016/S1876-3804(19)60235-1).
- Zhang, K., Sebakhy, K., Wu, K., Jing, G., Chen, N., Chen, Z., 2015. Future trends for tight oil exploitation. In: *SPE North Africa Technical Conference and Exhibition*. <https://doi.org/10.2118/175699-MS>.
- Zhao, M.W., Cheng, Y.L., Wu, Y.N., Dai, C.L., Gao, M.W., Yan, R.Q., Gao, X., 2022. Enhanced oil recovery mechanism by surfactant-silica nanoparticles imbibition in ultra-low permeability reservoirs. *J. Mol. Liq.* 348, 118010. <https://doi.org/10.1016/j.molliq.2021.118010>.
- Zhu, D.Y., Zhao, Y.H., Zhang, H.J., Zhao, Q., Shi, C.Y., Qin, J.H., Su, Z.H., Wang, G.Q., Liu, Y., Hou, J.R., 2023. Combined imbibition system with black nanosheet and low-salinity water for improving oil recovery in tight sandstone reservoirs. *Petrol. Sci.* 20, 1562–1571. <https://doi.org/10.1016/j.petsci.2022.12.004>.